

# EFFECT OF BEAMPATTERN ON MATRIX COMPLETION WITH SPARSE ARRAYS

Robin Rajamäki, Mehmet Can Hücümenoğlu, Pulak Sarangi, and Piya Pal

Department of Electrical and Computer Engineering, University of California San Diego

## ABSTRACT

We study the problem of noisy sparse array interpolation, where a large virtual array is synthetically generated by interpolating missing sensors using matrix completion techniques that promote low rank. The current understanding is quite limited regarding the effect of the (sparse) array geometry on the angle estimation error (post interpolation) of these methods. In this paper, we make advances towards solidifying this understanding by revealing the role of the *physical beampattern* of the sparse array on the performance of low rank matrix completion techniques. When the beampattern is analytically tractable (such as for uniform linear arrays and nested arrays), our analysis provides concrete and interpretable bounds on the scaling of the angular error as a function of the number of sensors, and demonstrates the effectiveness of nested arrays in presence of noise and a single temporal snapshot.

**Index Terms**— Sparse arrays, Matrix completion, Interpolation, Toeplitz, Positivite semidefinite.

## 1. INTRODUCTION

Sparse sensor arrays offer several advantages over conventional uniform arrays, such as enhanced angular resolution [1] and the ability to identify more sources than sensors [2]. Consequently, they hold great promise in a plethora of emerging applications, including mmWave channel estimation [3], automotive radar [4], and integrated sensing and communications (ISAC) [5]. A key challenge is to fully leverage the benefits of sparse arrays in sample-starved (even single-snapshot) [1, 6–12] scenarios. *Array interpolation* provides a potential remedy to these challenges [7]. In particular, matrix completion based approaches have gained significant attention [7, 9, 11] due to their ability to harness the *large filled aperture* of sparse arrays for high-resolution beamforming and direction-of-arrival estimation. Despite the surge of research on sparse array matrix completion, several theoretical questions remain open. Most notably, the impact of the physical array geometry on source localization error (post interpolation) is poorly understood. We address this outstanding issue by establishing that the *beampattern of sparse arrays* plays

a major role in matrix completion based array interpolation. We rigorously show that the *physical array beampattern* controls the worst-case error of these interpolation techniques, even when the goal is *not to perform beamforming*, but to estimate target parameters using other methods. Since beamforming is a linear operation, it is not *a priori* obvious that the beampattern should also directly influence the error of low-rank matrix completion—a *nonlinear* and *nonconvex* optimization problem. Although several nonlinear beamforming schemes [13–15] have been designed for sparse arrays, the connection between the (irregular) beampattern of sparse arrays and noisy matrix completion has not been investigated. Our results also offer an intuitive interpretation of the worst-case angular error (specifically, its scaling with the number of sensors) of any given array geometry in terms of the associated beampattern and its main lobe width (spatial resolution) / side lobe levels (noise robustness) with respect to the signal-to-noise ratio (SNR).

To make the connection concrete and for ease of exposition, we focus on a single source model with an unknown angle and (positive) amplitude. Single source models are relevant in, e.g., beam alignment for mmWave communication [16], as well as target detection and tracking for ISAC [5, pp. 122, 422]. The physical beampattern of sparse arrays will continue to play an important role for multiple (possibly real or complex-valued) sources. While such extensions are possible, they are not straightforward and are part of ongoing work.

*Notation:* Given matrix  $\mathbf{X} \in \mathbb{C}^{N \times M}$ ,  $\mathbf{X}_{\mathbb{X}}$  denotes the  $|\mathbb{X}| \times M$  matrix formed by retaining the  $|\mathbb{X}| \leq N$  rows indexed by set  $\mathbb{X} + 1 \subset \mathbb{N}_+$ . The Hermitian Toeplitz matrix whose first column is  $\mathbf{t} \in \mathbb{C}^N$  is denoted by  $\mathcal{T}(\mathbf{t}) \in \mathbb{C}^{N \times N}$ .

## 2. SIGNAL MODEL

Consider a  $P$ -sensor linear array with sensor positions given by set  $\mathbb{D} = \{d_1, d_2, \dots, d_P\} \subset \mathbb{N}$ ,  $d_1 = 0 < d_2 < \dots < d_P$  in units of half the carrier wavelength. We will focus on the uniform linear array (ULA),  $\mathbb{D} = \mathbb{U}_P \triangleq \{0, 1, \dots, P-1\}$ , and nested array [17],  $\mathbb{D} = \mathbb{S} \triangleq \mathbb{U}_M \cup ((M+1)\mathbb{U}_M + M)$ , where  $M \triangleq \frac{P}{2}$  and  $P$  is assumed even. Suppose we observe a single snapshot of a narrowband far field source signal with unknown angular direction  $\theta \in [-\frac{\pi}{2}, \frac{\pi}{2})$  and (positive) ampli-

This work was supported in part by grants ONR N00014-19-1-2256, NSF 2124929, and DE-SC0022165.

tude  $\alpha > 0$  impinging on the array in the presence of noise:

$$\mathbf{y} = \alpha \mathbf{a}_{\mathbb{D}}(\theta) + \mathbf{n}. \quad (1)$$

Here,  $\mathbf{a}_{\mathbb{D}}(\theta) \in \mathbb{C}^P$  is the steering vector satisfying  $[\mathbf{a}_{\mathbb{D}}(\theta)]_i = e^{j\pi d_i \sin \theta}$ ,  $d_i \in \mathbb{D}$  and noise is assumed to be bounded as  $\|\mathbf{n}\|_2 \leq \epsilon$ .

The objective of array interpolation is to emulate a large virtual ULA  $\mathbb{U}_N \supseteq \mathbb{D}$  with  $N \geq P$  sensors, by ‘‘computationally filling in’’ the missing sensors. A popular array interpolation approach is to solve a matrix completion problem [7–9, 18, 19] such as the following positive semidefinite (PSD) Toeplitz completion problem:

$$\underset{\mathbf{t} \in \mathbb{C}^N}{\text{minimize}} \text{rank } \mathcal{T}(\mathbf{t}) \text{ s.t. } \|\mathbf{y} - \mathbf{t}_{\mathbb{D}}\|_2 \leq \epsilon, \mathcal{T}(\mathbf{t}) \succeq 0. \quad (\text{P0})$$

In the following, we denote the steering vector of  $\mathbb{U}_N$  by  $\mathbf{a}(\theta) \in \mathbb{C}^N$ , where  $a_i(\theta) = e^{j\pi(i-1)\sin \theta}$ ,  $i = 1, 2, \dots, N$ . Hence,  $\mathbf{a}_{\mathbb{D}}(\theta) \in \mathbb{C}^P$  can be interpreted as consisting of a subset of the entries of  $\mathbf{a}(\theta)$ , sampled by  $\mathbb{D}$ .

**Proposition 1 (Rank-1 solutions).** *Suppose  $\mathbf{y} = \alpha \mathbf{a}_{\mathbb{D}}(\theta) + \mathbf{n}$ , where  $\|\mathbf{n}\|_2 \leq \epsilon$  and  $\alpha > 2\epsilon/\sqrt{P}$ . Then any solution  $\hat{\mathbf{t}} \in \mathbb{C}^N$  to (P0) is of the form  $\hat{\mathbf{t}} = \hat{\alpha} \mathbf{a}(\hat{\theta})$ ,  $\hat{\alpha} > 0$ .*

*Proof.* Let  $\hat{\mathbf{t}}$  be a minimizer of (P0). Note that  $\mathbf{t}' = \alpha \mathbf{a}(\theta)$  is a feasible point, since  $\mathcal{T}(\mathbf{t}') = \alpha \mathbf{a}(\theta) \mathbf{a}^H(\theta)$  is PSD and  $\|\mathbf{y} - \alpha \mathbf{a}_{\mathbb{D}}(\theta)\|_2 = \|\mathbf{n}\|_2 \leq \epsilon$ . Hence, there exists a feasible point satisfying  $\text{rank}(\mathcal{T}(\mathbf{t}')) = 1$ . This is also the minimum rank solution, since a zero-rank solution is infeasible due to the assumption  $\alpha > 2\epsilon/\sqrt{P}$ . Finally, as  $\mathcal{T}(\hat{\mathbf{t}})$  is a rank-1 PSD Toeplitz matrix, it admits Vandermonde decomposition  $\mathcal{T}(\hat{\mathbf{t}}) = \hat{\alpha} \mathbf{a}(\hat{\theta}) \mathbf{a}^H(\hat{\theta})$  by Caratheodory’s theorem [20]. Hence,  $\hat{\mathbf{t}} = \hat{\alpha} \mathbf{a}(\hat{\theta})$ ,  $\hat{\alpha} > 0$ .  $\square$

Proposition 1 establishes that for large enough  $\alpha$ , any solution to (P0) will have the parametric form  $\hat{\mathbf{t}} = \hat{\alpha} \mathbf{a}(\hat{\theta})$  which represents a scaled virtual steering vector corresponding to angle  $\hat{\theta}$ . Consequently, the remainder of this paper focuses on the angle estimation error of the *class of estimators that use  $\hat{\theta}$  as an estimate of  $\theta$* . Prominent members of this class include beamforming and subspace methods [21, 22] that operate on  $\hat{\mathbf{t}}$ .<sup>1</sup> The following question underlies our main contribution: ‘‘Is it possible to obtain a universal upper bound on the angle estimation error for this class?’’ If so, what is the quantity of interest (specific to an array geometry) that determines such a bound? Interestingly, an answer is given by the so-called *unweighted physical array beampattern*.

<sup>1</sup>Beamforming seeks  $\arg \max_{\vartheta} |\alpha^H(\vartheta) \hat{\mathbf{t}}| = \arg \max_{\vartheta} \hat{\alpha} |\alpha^H(\vartheta) \mathbf{a}(\hat{\theta})| = \hat{\theta}$ , whereas subspace methods find  $\hat{\theta}$  by identifying the (rank-1) subspace spanned by  $\mathbf{a}(\hat{\theta})$  from  $\mathcal{T}(\hat{\mathbf{t}}) = \hat{\alpha} \mathbf{a}(\hat{\theta}) \mathbf{a}^H(\hat{\theta})$ .

### 3. BEAMPATTERN AND ANGULAR ERROR OF MATRIX COMPLETION

The *unweighted beamformer* of array  $\mathbb{D}$  for spatial frequency  $\omega \in \mathbb{R}$  is given by

$$H_{\mathbb{D}}(\omega) \triangleq \sum_{d \in \mathbb{D}} e^{j\pi d \omega}. \quad (2)$$

For any nonzero solution of (P0),  $\hat{\mathbf{t}} = \hat{\alpha} \mathbf{a}(\hat{\theta}) \in \mathbb{C}^N$ , we have

$$\|\mathbf{y} - \hat{\mathbf{t}}_{\mathbb{D}}\|_2 = \|\alpha \mathbf{a}_{\mathbb{D}}(\theta) - \hat{\alpha} \mathbf{a}_{\mathbb{D}}(\hat{\theta}) + \mathbf{n}\|_2 = \|\mathbf{A}_{\mathbb{D}} \boldsymbol{\alpha} + \mathbf{n}\|_2,$$

where  $\mathbf{A}_{\mathbb{D}} \triangleq [\mathbf{a}_{\mathbb{D}}(\theta), \mathbf{a}_{\mathbb{D}}(\hat{\theta})]$  and  $\boldsymbol{\alpha} \triangleq [\alpha, -\hat{\alpha}]^T$ . Hence,

$$\epsilon \geq \|\mathbf{y} - \hat{\mathbf{t}}_{\mathbb{D}}\|_2 \geq \|\mathbf{A}_{\mathbb{D}} \boldsymbol{\alpha}\|_2 - \|\mathbf{n}\|_2 \geq \sigma_2(\mathbf{A}_{\mathbb{D}}) \|\boldsymbol{\alpha}\|_2 - \epsilon. \quad (3)$$

Here  $\sigma_2(\mathbf{A}_{\mathbb{D}})$  denotes the second largest singular value of  $\mathbf{A}_{\mathbb{D}}$ . The last inequality holds whenever  $\mathbf{A}_{\mathbb{D}}$  has full column rank, which can be verified to be true for ULAs and nested arrays when  $M \geq 2$ . Rearranging (3) yields

$$\sigma_2(\mathbf{A}_{\mathbb{D}}) \leq \frac{2\epsilon}{\sqrt{\alpha^2 + \hat{\alpha}^2}} \leq 2 \frac{\epsilon}{\alpha} = 2\rho^{-1/2}, \quad (4)$$

where  $\rho \triangleq (\alpha/\epsilon)^2$  is defined as the SNR. Now, let  $\bar{\omega} \triangleq \sin \hat{\theta} - \sin \theta$ , and note that

$$\sigma_2^2(\mathbf{A}_{\mathbb{D}}) = \sigma_2(\mathbf{A}_{\mathbb{D}}^H \mathbf{A}_{\mathbb{D}}) = \sigma_2 \left( \begin{bmatrix} P & H_{\mathbb{D}}(\bar{\omega}) \\ H_{\mathbb{D}}^*(\bar{\omega}) & P \end{bmatrix} \right),$$

since  $\mathbf{a}_{\mathbb{D}}^H(\theta) \mathbf{a}_{\mathbb{D}}(\hat{\theta}) = H_{\mathbb{D}}(\bar{\omega})$ . The characteristic polynomial of  $\mathbf{A}_{\mathbb{D}}^H \mathbf{A}_{\mathbb{D}}$  has two (non-negative) roots, the smaller one being

$$\sigma_2^2(\mathbf{A}_{\mathbb{D}}) = P - |H_{\mathbb{D}}(\bar{\omega})|. \quad (5)$$

This establishes the correspondence between the *beampattern*  $|H_{\mathbb{D}}(\bar{\omega})|$  and the second largest singular value of  $\mathbf{A}_{\mathbb{D}}$ . For convenience, instead of  $\bar{\omega} \in (-2, 2)$ , we henceforth consider the *wrap-around distance*  $\Delta \in [0, 1]$ , defined as

$$\Delta \triangleq \min_{k \in \mathbb{Z}} |\sin \hat{\theta} - \sin \theta + 2k|. \quad (6)$$

It can be verified that  $|H_{\mathbb{D}}(\Delta)| = |H_{\mathbb{D}}(\bar{\omega})|$ . Thus, by (4) to (6)

$$\frac{1}{P} |H_{\mathbb{D}}(\Delta)| \geq 1 - \frac{4}{P\rho}. \quad (7)$$

Eq. (7) yields a useful *necessary* condition that the angular error  $\Delta$  of any solution to (P0) must satisfy. A key insight offered by (7) is that a low  $\Delta$  is guaranteed if the SNR  $\rho$  is within the *main lobe* of the beampattern. This implies that properly designed sparse arrays can achieve much lower angular error than the ULA, provided the side lobes of the sparse array are not too high. Fig. 1 illustrates these observations in case of three arrays with  $P = 10$  sensors: the ULA  $\mathbb{D} = \mathbb{U}_{10}$ , dilated ULA  $\mathbb{D} = 3\mathbb{U}_{10}$ , and nested array  $\mathbb{D} = \mathbb{U}_5 \cup (6\mathbb{U}_5 + 5)$ . Note that (7) is independent of  $N$ . This is consistent with the notion that extrapolation cannot fundamentally decrease angular error. Finally, extensions to  $K > 1$  sources require ensuring that the solution to (P0) is of rank  $K$ , and characterizing the smallest singular value of a  $2K \times 2K$  matrix.

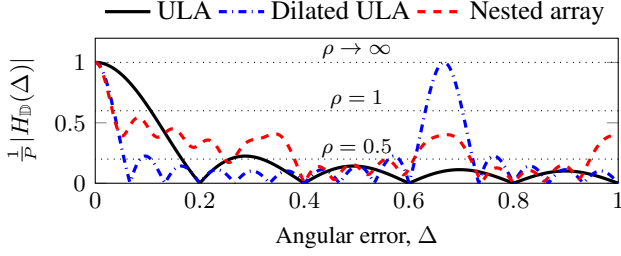


**Fig. 1.** Beampattern  $|H_{\mathbb{D}}(\Delta)|$  and SNR  $\rho$  control angular error  $\Delta$  of matrix completion. Horizontal dotted lines indicate the right hand side of (7) for different values of  $\rho$ . When  $\rho$  is sufficiently large,  $\Delta$  is determined by the intersection of the corresponding horizontal line with the main lobe, which is narrower for sparse arrays. However, low side lobes are also necessary to guarantee low  $\Delta$ .

#### 4. ANALYTICAL UPPER BOUNDS ON ANGULAR ERROR

Fig. 1 showed that simply plotting the (irregular) beampattern of an arbitrary sparse array is a practical means of deducing an upper bound on the angular error  $\Delta$ . Since  $|H_{\mathbb{D}}(\Delta)|$  can be a complicated function of  $\Delta$ , analytically inverting it is challenging in general. However, for certain structured arrays,  $|H_{\mathbb{D}}(\Delta)|$  becomes analytically tractable, which helps in characterizing the scaling of  $\Delta$  with parameters of interest such as  $P$ . Let  $\Delta_{\mathbb{D}}$  denote the angle estimation error resulting from solving (P0) and using any estimator from the class discussed in Section 2. The following theorem provides upper bounds on  $\Delta_{\mathbb{D}}$  which reveal how fast the error decays with  $P$ .

**Theorem 1.** *Let  $P = 2M$ , where  $M \geq 2$ . If  $\rho \geq 25/P$ , then  $\Delta_{\mathbb{U}_P} \leq 1.2/P$  and  $\Delta_{\mathbb{S}} \leq 8/P^2$ .*

*Proof. ULA:* By basic properties of geometric series and trigonometric identities,  $|H_{\mathbb{U}_m}(\Delta)| = \left| \frac{\sin(\pi m \Delta/2)}{\sin(\pi \Delta/2)} \right|$ . Following  $|\sin y| \leq |y|, \forall y$  and  $\sin y \geq \frac{2}{\pi}y, y \in (0, \frac{\pi}{2}]$  [23, p. 33],

$$|H_{\mathbb{U}_m}(\Delta)| \leq \min \left( m, \frac{1}{\Delta} \right) \quad 0 < \Delta \leq 1. \quad (8)$$

Since (7) holds for all feasible solutions, it is also true for the worst-case error  $\Delta_{\mathbb{U}_P}$ . Combining this with  $\rho \geq 25/P$ :

$$\begin{aligned} \frac{1}{P\Delta_{\mathbb{U}_P}} &\geq \frac{1}{P}|H_{\mathbb{U}_P}(\Delta_{\mathbb{U}_P})| \geq 1 - \frac{4}{P\rho} \geq 1 - \frac{4}{25} = \frac{21}{25} \\ \implies \Delta_{\mathbb{U}_P} &\leq \frac{25/21}{P} \leq \frac{1.2}{P}. \end{aligned}$$

Nested Array: The nested array can be written as  $\mathbb{S} = \mathbb{S}_1 \cup \mathbb{S}_2$  where  $\mathbb{S}_1 \triangleq \mathbb{U}_M$  and  $\mathbb{S}_2 \triangleq (M+1)\mathbb{U}_M + M$  are

disjoint sets. Hence, by the triangle inequality,

$$\begin{aligned} |H_{\mathbb{S}}(\Delta)| &= \left| \sum_{d_1 \in \mathbb{S}_1} e^{j\pi d_1 \Delta} + \sum_{d_2 \in \mathbb{S}_2} e^{j\pi d_2 \Delta} \right| \\ &= \left| \sum_{i=1}^M e^{j\pi(i-1)\Delta} + e^{j\pi M \Delta} \sum_{i=1}^M e^{j\pi(i-1)(M+1)\Delta} \right| \\ &\leq |H_{\mathbb{U}_M}(\Delta)| + |H_{\mathbb{U}_M}((M+1)\Delta)|. \end{aligned} \quad (9)$$

Alternatively,  $\mathbb{S} = \mathbb{S}'_1 \cup \mathbb{S}'_2$  where  $\mathbb{S}'_1 \triangleq \mathbb{U}_{M+1}$ ,  $\mathbb{S}'_2 \triangleq (M+1)\mathbb{U}_{M-1} + 2M+1$ , and  $\mathbb{S}'_1 \cap \mathbb{S}'_2 = \emptyset$ . Hence, similarly to (9),

$$|H_{\mathbb{S}}(\Delta)| \leq |H_{\mathbb{U}_{M+1}}(\Delta)| + |H_{\mathbb{U}_{M-1}}((M+1)\Delta)|. \quad (10)$$

We proceed by showing that the worst-case angle error obeys  $|H_{\mathbb{S}}(\Delta_{\mathbb{S}})| < 0.84P$  when  $\Delta_{\mathbb{S}} \in [\frac{2}{(M+1)M}, 1]$ , which can be interpreted as upper bounding the highest side lobe level. We consider two subintervals:

- (i)  $\Delta_{\mathbb{S}} \in [\frac{2}{(M+1)M}, \frac{1}{M+1}]$ : Denote  $\Delta' = \Delta_{\mathbb{S}}(M+1)$ . Thus,  $\Delta' \in [\frac{2}{M}, 1)$ , which by (8) implies that

$$|H_{\mathbb{U}_M}((M+1)\Delta_{\mathbb{S}})| = |H_{\mathbb{U}_M}(\Delta')| \leq \frac{1}{\Delta'} \leq \frac{M}{2}.$$

Hence,  $|H_{\mathbb{S}}(\Delta_{\mathbb{S}})| \leq M + \frac{M}{2} = \frac{3P}{4}$  by (8) and (9).

- (ii)  $\Delta_{\mathbb{S}} \in [\frac{1}{M+1}, 1]$ : Note that  $\sin(\pi \Delta_{\mathbb{S}}/2)$  is a positive increasing function of  $\Delta_{\mathbb{S}}$  when  $\Delta_{\mathbb{S}} \in [\frac{1}{M+1}, 1]$ . Thus,  $\frac{1}{\sin(\pi \Delta_{\mathbb{S}}/2)} \leq \frac{1}{\sin(\pi/(2(M+1)))}$ . Moreover,  $\sin x \geq (1 - \frac{x^2}{6})x, x \in [0, \frac{\pi}{2}]$  can be established using the Taylor series expansion of  $\sin x$  [24, Eq. (3.1)]. Applying these two facts to  $|H_{\mathbb{U}_{M+1}}(\Delta_{\mathbb{S}})|$  yields

$$|H_{\mathbb{U}_{M+1}}(\Delta_{\mathbb{S}})| \leq \frac{1}{\sin(\frac{\pi/2}{M+1})} \leq \frac{(M+1)12/\pi}{6 - (\frac{\pi/2}{M+1})^2}. \quad (11)$$

Recalling assumption  $M \geq 2$ , we substitute  $M = 2$  in the denominator of (11)—an increasing function of  $M$ —to obtain  $|H_{\mathbb{U}_{M+1}}(\Delta_{\mathbb{S}})| < 0.67(M+1)$ . Thus by (10) and (8):  $|H_{\mathbb{S}}(\Delta_{\mathbb{S}})| < 0.67(M+1) + M - 1 < 1.67M < 0.84P$ .

In summary, if  $\Delta_{\mathbb{S}} \geq \frac{2}{(M+1)M}$  then  $\frac{1}{P}|H_{\mathbb{S}}(\Delta_{\mathbb{S}})| < \max(\frac{3}{4}, 0.84) = 0.84$ . Also note that  $\frac{1}{P}|H_{\mathbb{S}}(\Delta_{\mathbb{S}})| = 1 > 0.84$  when  $\Delta_{\mathbb{S}} = 0$ . This shows that if  $\frac{1}{P}|H_{\mathbb{S}}(\Delta_0)| > 0.84$  for some  $\Delta_0$ , then it must hold that  $\Delta_0 \in [0, \frac{2}{(M+1)M}]$ . Theorem 1 now follows via contradiction: Let  $\rho \geq 25/P$ . Suppose  $\Delta_{\mathbb{S}} \geq \frac{2}{(M+1)M}$ . However, by (7):  $0.84 > \frac{1}{P}|H_{\mathbb{S}}(\Delta_{\mathbb{S}})| \geq 1 - \frac{4}{P\rho} \geq 1 - \frac{4}{25} = 0.84$ , which is a contradiction. Hence, if  $\rho \geq 25/P$  then  $\Delta_{\mathbb{S}} < \frac{2}{(M+1)M} \leq \frac{2}{M^2} = \frac{8}{P^2}$ . This completes the proof.  $\square$

Theorem 1 reveals an interesting fact: when the SNR is at least proportional to  $\frac{1}{P}$ , the upper bound on the worst-case

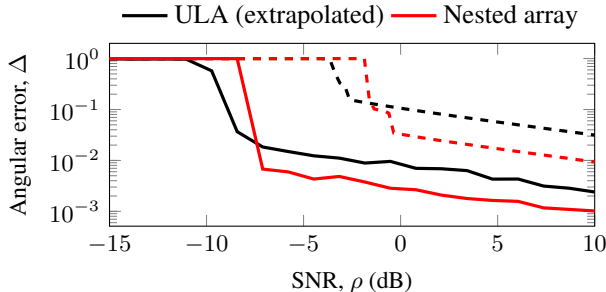


**Fig. 2.** Angular error of matrix completion as a function of SNR  $\rho$  (for  $P = 10$ ). The empirical error (solid) follows the trends of the upper bounds derived from (7) (dashed curves).

angle estimation error decays with  $P$  at different rates for the ULA and the nested array. The more favorable decay of the bound in case of the nested array— $\frac{1}{P^2}$  compared to  $\frac{1}{P}$  for the ULA—can also be attributed to the narrower main lobe of its beampattern, as discussed in Section 3.

## 5. NUMERICAL EXPERIMENTS

This section numerically validates the theory outlined in Sections 3 and 4. We solve a well-known convex relaxation of (P0), where instead of the rank, we minimize the trace<sup>2</sup> of  $\mathcal{T}(\mathbf{t})$  using the CVX toolbox [25]. We obtain an estimate  $\hat{\theta}$  of angle  $\theta$  by applying root-MUSIC [26] on  $\mathcal{T}(\hat{\mathbf{t}})$ . We repeat this experiment for 1000 Monte Carlo trials, where both the ground truth  $\sin \theta$ , and the real and imaginary parts of the entries of noise vector  $\mathbf{n}$  are drawn independently at random from a uniform distribution, such that  $\sin \theta, \frac{\epsilon}{\sqrt{2P}} \Re\{n_i\}, \frac{\epsilon}{\sqrt{2P}} \Im\{n_i\} \sim \mathcal{U}(-1, 1), i = 1, 2, \dots, N$ . We fix  $\alpha = 1$ . SNR is varied by only varying the noise level  $\epsilon$ .

Fig. 2 shows the angular error  $\Delta$  as a function of SNR  $\rho$  for the extrapolated ULA and nested array with  $P = 10$  sensors and  $N = 30$  (aperture of the nested array). An upper bound on  $\Delta$  (dashed curves) computed using (7) and the array beampatterns in Fig. 1, and the largest value of  $\Delta$  observed over the Monte Carlo trials (solid curves) display similar trends and scaling with respect to the array geometries and  $\rho$ . This demonstrates the utility of (7) for predicting the angular error of matrix completion for diverse array configurations. Fig. 2 shows an initial sharp transition from high to low error, which corresponds to the transition from the side lobe region to the mainlobe of the beampattern (cf. Fig. 1). The (extrapolated) ULA seems to display an advantage in a narrow range of low SNR values, which can be attributed to its lower peak side lobe level. However, as SNR increases, the nested array achieves a consistently lower angular error thanks to its narrower main lobe, *despite* the fact that the ULA is extrapolated to the same virtual aperture (since  $N = 30$ ).

<sup>2</sup>Since  $\mathcal{T}(\mathbf{t})$  is PSD, minimizing the trace is equivalent to minimizing the nuclear norm (sum of singular values) or simply the first entry of vector  $\mathbf{t}$ .

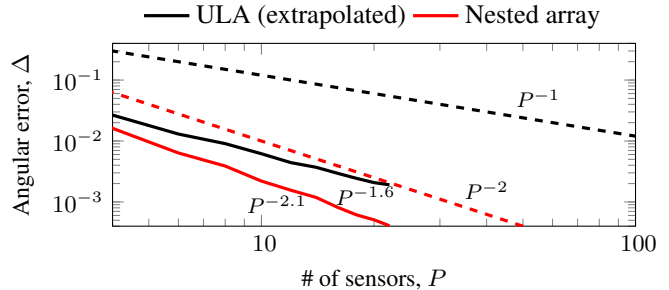


**Fig. 3.** Angular error of matrix completion as a function of the number of sensors  $P$  (for  $\rho = \frac{16}{P}$ ). For  $P \in [4, 22]$ , the empirical curves (solid) decay slightly faster than the scaling laws  $\frac{1}{P}$  and  $\frac{1}{P^2}$  predicted by Theorem 1 (dashed lines).

Fig. 3 shows the scaling of the worst-case value of  $\Delta$  as a function of the number of sensors  $P$  when the SNR scales as  $\rho = 16/P$ . The angular error of the nested array decays faster with  $P$  compared to the extrapolated ULA both in case of the trends predicted by Theorem 1 (dashed lines), and the empirical maximum error over the Monte Carlo trials using trace minimization and root-MUSIC (solid lines). Fig. 3 also displays the approximate rates of decay estimated by a least-squares fit of linear model  $\log \Delta = a \log P + b$  to the empirical curves. Over interval  $P = 4, 6, \dots, 22$ , a faster decay is observed experimentally— $P^{-1.6}$  (ULA) and  $P^{-2.1}$  (nested array)—compared to Theorem 1 ( $P^{-1}$  and  $P^{-2}$ ). Whether this trend persists for larger values of  $P$ , or for other optimization algorithms and noise models is still an open question.

## 6. CONCLUSIONS

We showed that the sparse array beampattern fundamentally controls the angular error of array interpolation based on matrix completion. Specifically, we derived upper bounds on the error of angle estimates revealed by solutions to a low rank Toeplitz completion problem, where noisy measurements of a single unknown (positive) source signal are observed. Using this insight, we proved that nested arrays can attain lower worst-case angle estimation error than ULAs (extrapolated to the same aperture) for comparable SNR. The theoretical findings were supported by numerical experiments that corroborate the advantages of sparse arrays compared to uniform arrays in noisy sample-starved regimes.

## 7. REFERENCES

- [1] P. Sarangi, M. C. Hücümenoğlu, R. Rajamäki, and P. Pal, “Super-resolution with sparse arrays: A nonasymptotic analysis of spatiotemporal trade-offs,” *IEEE Transactions on Signal Processing*, vol. 71, pp. 4288–4302, 2023.
- [2] M. Wang and A. Nehorai, “Coarrays, MUSIC, and the

- Cramér-Rao bound,” *IEEE Transactions on Signal Processing*, vol. 65, no. 4, pp. 933–946, Feb 2017.
- [3] S. Haghghatshoar and G. Caire, “Low-complexity massive MIMO subspace estimation and tracking from low-dimensional projections,” *IEEE Trans. on Signal Processing*, vol. 66, no. 7, pp. 1832–1844, 2018.
- [4] S. M. Patole, M. Torlak, D. Wang, and M. Ali, “Automotive radars: A review of signal processing techniques,” *IEEE Signal Processing Magazine*, vol. 34, no. 2, pp. 22–35, 2017.
- [5] F. Liu, C. Masouros, and Y. C. Eldar, *Integrated Sensing and Communications*. Springer Singapore, 2023.
- [6] P. Sarangi, M. C. Hücümenoğlu, and P. Pal, “Beyond coarray MUSIC: Harnessing the difference sets of nested arrays with limited snapshots,” *IEEE Signal Processing Letters*, vol. 28, pp. 2172–2176, 2021.
- [7] —, “Single-snapshot nested virtual array completion: Necessary and sufficient conditions,” *IEEE Signal Processing Letters*, vol. 29, pp. 2113–2117, 2022.
- [8] M. C. Hücümenoğlu, P. Sarangi, R. Rajamäki, and P. Pal, “To regularize or not to regularize: The role of positivity in sparse array interpolation with a single snapshot,” in *IEEE International Conference on Acoustics, Speech and Signal Processing (ICASSP)*, 2023, pp. 1–5.
- [9] S. Sun and A. P. Petropulu, “A sparse linear array approach in automotive radars using matrix completion,” in *IEEE International Conference on Acoustics, Speech and Signal Processing (ICASSP)*, 2020, pp. 8614–8618.
- [10] S. Liu, Z. Mao, Y. D. Zhang, and Y. Huang, “Rank minimization-based Toeplitz reconstruction for DoA estimation using coprime array,” *IEEE Communications Letters*, vol. 25, no. 7, pp. 2265–2269, 2021.
- [11] M. Bokaei, S. Razavikia, A. Amini, and S. Rini, “Single-snapshot DOA estimation via weighted Hankel-structured matrix completion,” in *2022 30th European Signal Processing Conference (EUSIPCO)*, 2022, pp. 1756–1760.
- [12] Y. Ma, X. Cao, X. Wang, M. S. Greco, and F. Gini, “Multi-source off-grid DOA estimation with single snapshot using non-uniform linear arrays,” *Signal Processing*, vol. 189, p. 108238, 2021.
- [13] P. P. Vaidyanathan and P. Pal, “Sparse sensing with coprime samplers and arrays,” *IEEE Transactions on Signal Processing*, vol. 59, no. 2, pp. 573–586, Feb 2011.
- [14] K. Adhikari and J. R. Buck, “Spatial spectral estimation with product processing of a pair of colinear arrays,” *IEEE Transactions on Signal Processing*, vol. 65, no. 9, pp. 2389–2401, 2017.
- [15] R. Cohen and Y. C. Eldar, “Sparse convolutional beamforming for ultrasound imaging,” *IEEE Transactions on Ultrasonics, Ferroelectrics, and Frequency Control*, vol. 65, no. 12, pp. 2390–2406, Dec 2018.
- [16] S.-E. Chiu, N. Ronquillo, and T. Javidi, “Active learning and CSI acquisition for mmWave initial alignment,” *IEEE Journal on Selected Areas in Communications*, vol. 37, no. 11, pp. 2474–2489, 2019.
- [17] P. Pal and P. P. Vaidyanathan, “Nested arrays: A novel approach to array processing with enhanced degrees of freedom,” *IEEE Transactions on Signal Processing*, vol. 58, no. 8, pp. 4167–4181, Aug 2010.
- [18] Y. Abramovich, N. Spencer, and A. Gorokhov, “Positive-definite Toeplitz completion in DOA estimation for nonuniform linear antenna arrays. II. partially augmentable arrays,” *IEEE Transactions on Signal Processing*, vol. 47, no. 6, pp. 1502–1521, 1999.
- [19] H. Qiao and P. Pal, “Unified analysis of co-array interpolation for direction-of-arrival estimation,” in *IEEE International Conference on Acoustics, Speech and Signal Processing (ICASSP)*, March 2017, pp. 3056–3060.
- [20] G. Cybenko, “Moment problems and low rank Toeplitz approximations,” *Circuits, Systems and Signal Processing*, vol. 1, pp. 345–366, 1982.
- [21] W. Liao and A. Fannjiang, “MUSIC for single-snapshot spectral estimation: Stability and super-resolution,” *Applied and Computational Harmonic Analysis*, vol. 40, no. 1, pp. 33–67, 2016.
- [22] W. Li, W. Liao, and A. Fannjiang, “Super-resolution limit of the ESPRIT algorithm,” *IEEE transactions on information theory*, vol. 66, no. 7, pp. 4593–4608, 2020.
- [23] D. S. Mitrinovic and P. M. Vasic, *Analytic inequalities*. Springer, 1970, vol. 1.
- [24] R. Klén, M. Visuri, and M. Vuorinen, “On Jordan type inequalities for hyperbolic functions,” *Journal of Inequalities and Applications*, vol. 2010, pp. 1–14, 2010.
- [25] M. Grant and S. Boyd, “CVX: Matlab software for disciplined convex programming, version 2.2,” <http://cvxr.com/cvx>, Mar. 2014.
- [26] A. Barabell, “Improving the resolution performance of eigenstructure-based direction-finding algorithms,” in *IEEE International Conference on Acoustics, Speech, and Signal Processing (ICASSP)*, vol. 8, 1983, pp. 336–339.